



Year: 2013

In vivo imaging of prostate cancer using [68Ga]-labeled bombesin analog BAY86-7548

Kähkönen, Esa ; Jambor, Ivan ; Kemppainen, Jukka ; Lehtiö, Kaisa ; Grönroos, Tove J ; Kuisma, Anna ; Luoto, Pauliina ; Sipilä, Henri J ; Tolvanen, Tuula ; Alanen, Kalle ; Silén, Jonna ; Kallajoki, Markku ; Roivainen, Anne ; Schäfer, Niklaus ; Schibli, Roger ; Dragic, Martina ; Johayem, Anass ; Valencia, Ray ; Borkowski, Sandra ; Minn, Heikki

Abstract: PURPOSE: A novel [(68)Ga]-labeled DOTA-4-amino-1-carboxymethyl-piperidine-D-Phe-Gln-Trp-Ala-Val-Gly-His-Sta-Leu-NH₂ peptide (BAY86-7548) having high affinity to bombesin receptor sub-type II to detect primary and metastatic prostate carcinoma using positron emission tomography/computed tomography (PET/CT) was synthesized and evaluated for prostate cancer. **EXPERIMENTAL DESIGN:** In this first human study with BAY86-7548, 14 men scheduled for radical prostatectomy (n = 11) or with biochemical recurrence after surgery or hormonal therapy (n = 3) were enrolled. The patients received an intravenous injection of BAY86-7548 followed by over 60-minute dynamic imaging of prostate gland (n = 10) and/or subsequent whole-body imaging (n = 14). The visual assessment of PET/CT images included evaluation of intraprostatic (12 subsectants) and pelvic nodal uptake of BAY86-7548 in 11 surgical patients and detection of potential metastatic foci in all patients. In patients with biochemical recurrence, results were compared with those of either [(11)C]-acetate (n = 2) or [(18)F]-fluoromethylcholine (n = 1) PET/CT. **RESULTS:** We found a sensitivity, specificity, and accuracy of 88%, 81% and 83%, respectively, for detection of primary PCa and sensitivity of 70% for metastatic lymph nodes using histology as gold standard. BAY86-7548 correctly detected local recurrence in prostate bed and showed nodal relapse in accordance with [(11)C]-acetate PET/CT in 2 patients with biochemical relapse. In the third hormone refractory patient, BAY86-7548 failed to show multiple bone metastases evident on [(18)F]-fluoromethylcholine PET/CT. **CONCLUSION:** BAY86-7548 PET/CT is a promising molecular imaging technique for detecting intraprostatic prostate cancer.

DOI: <https://doi.org/10.1158/1078-0432.CCR-12-3490>

Posted at the Zurich Open Repository and Archive, University of Zurich

ZORA URL: <https://doi.org/10.5167/uzh-91910>

Journal Article

Accepted Version

Originally published at:

Kähkönen, Esa; Jambor, Ivan; Kemppainen, Jukka; Lehtiö, Kaisa; Grönroos, Tove J; Kuisma, Anna; Luoto, Pauliina; Sipilä, Henri J; Tolvanen, Tuula; Alanen, Kalle; Silén, Jonna; Kallajoki, Markku; Roivainen, Anne; Schäfer, Niklaus; Schibli, Roger; Dragic, Martina; Johayem, Anass; Valencia, Ray; Borkowski, Sandra; Minn, Heikki (2013). In vivo imaging of prostate cancer using [68Ga]-labeled bombesin analog BAY86-7548. *Clinical Cancer Research*, 19(19):5434-5443.

DOI: <https://doi.org/10.1158/1078-0432.CCR-12-3490>

Clinical Cancer Research



In vivo imaging of prostate cancer using [^{68}Ga]-labeled bombesin analog BAY86-7548

Esa Kahkonen, Ivan Jambor, Jukka Kempainen, et al.

Clin Cancer Res Published OnlineFirst August 9, 2013.

Updated version Access the most recent version of this article at:
doi:[10.1158/1078-0432.CCR-12-3490](https://doi.org/10.1158/1078-0432.CCR-12-3490)

Author Manuscript Author manuscripts have been peer reviewed and accepted for publication but have not yet been edited.

E-mail alerts [Sign up to receive free email-alerts](#) related to this article or journal.

Reprints and Subscriptions To order reprints of this article or to subscribe to the journal, contact the AACR Publications Department at pubs@aacr.org.

Permissions To request permission to re-use all or part of this article, contact the AACR Publications Department at permissions@aacr.org.

In Vivo Imaging of Prostate Cancer Using [⁶⁸Ga]-Labeled Bombesin Analog BAY86-7548

Esa Kähkönen^{1*}, Ivan Jambor^{2,3*}, Jukka Kemppainen^{2,4}, Kaisa Lehtiö⁵, Tove J. Grönroos², Anna Kuisma⁵, Pauliina Luoto², Henri J. Sipilä², Tuula Tolvanen², Kalle Alanen⁶, Jonna Silén², Markku Kallajoki⁶, Anne Roivainen², Niklaus Schäfer⁷, Roger Schibli⁸, Martina Dragic⁸, Anass Johayem⁹, Ray Valencia¹⁰, Sandra Borkowski¹⁰, Heikki Minn^{2,5}

** Equal contribution*

¹ Department of Surgery, Division of Urology, Turku University Hospital, Turku, Finland

² Turku PET Centre, University of Turku, Turku, Finland

³ Department of Diagnostic Radiology, University of Turku, Turku, Finland

⁴ Department of Clinical Physiology and Nuclear Medicine, Turku University Hospital, Turku, Finland

⁵ Department of Oncology and Radiotherapy, Turku University Hospital, Turku, Finland

⁶ Department of Pathology, Turku University Hospital, Turku, Finland

⁷ Department of Medical Oncology and Nuclear Medicine, University Hospital of Zurich, Zurich, Switzerland

⁸ Department of Chemistry and Applied Biosciences, ETH Zurich, Zurich, Switzerland

⁹ Department of Nuclear Medicine, University Hospital of Zurich, Zurich, Switzerland

¹⁰ Bayer Pharma AG, Berlin, Germany

Running title:

[⁶⁸Ga]-bombesin analog BAY86-7548 PET/CT in prostate cancer

Keywords:

Prostate cancer, PET/CT, bombesin receptor analogs, [⁶⁸Ga]-labeled tracer, BAY86-7548

Financial support:

This study was sponsored by Bayer Pharma AG, Berlin, Germany

Corresponding author:

Heikki Minn, MD, PhD

Department of Oncology and Radiotherapy, University of Turku

Kiinamyllynkatu 4-8

P.O. Box 52

FI-20521 Turku

Tel: +358 2 313 0149

Fax: +358 2 313 2809

Email: [heminn@utu.fi](mailto:heminm@utu.fi)

Conflict of interest:

Ray Valencia and Sandra Borkowski are employed by Bayer Pharma AG, Berlin, Germany.

No other possible conflicts of interest are present. Last author had full access to all the data in the study and takes responsibility for the integrity of the data and the accuracy of the data analysis.

Word count: 5499

Number of figures: 5

Number of tables: 1

Abstract

Purpose:

A novel [^{68}Ga]-labeled DOTA-4-amino-1-carboxymethyl-piperidine-*D*-Phe-Gln-Trp-Ala-Val-Gly-His-Sta-Leu-NH₂ peptide (BAY86-7548) having high affinity to bombesin receptor subtype 2 to detect primary and metastatic prostate carcinoma (PCa) using PET/CT was synthesized and evaluated for prostate cancer (PCa).

Experimental Design:

In this first human study with BAY86-7548, fourteen men scheduled for radical prostatectomy (n=11) or with biochemical recurrence after surgery or hormonal therapy (n=3) were enrolled. The patients received an intravenous injection of BAY86-7548 followed by over 60-minute dynamic imaging of prostate gland (n=10) and/or subsequent whole-body imaging (n=14). The visual assessment of PET/CT images included evaluation of intraprostatic (12 subsectants) and pelvic nodal uptake of BAY86-7548 in 11 surgical patients and detection of potential metastatic foci in all patients. In patients with biochemical recurrence, results were compared to those of either [^{11}C]-acetate (n=2) or [^{18}F]-fluoromethylcholine (n=1) PET/CT.

Results:

Using histology as gold standard, an increase in sensitivity, specificity, and accuracy for detection of primary PCa was observed (88%, 81% and 83%, respectively). In addition, sensitivity for detecting metastatic lymph nodes was increased by 70%. BAY86-7548 correctly detected local recurrence in prostate bed and showed nodal relapse in accordance with [^{11}C]-acetate PET/CT in two patients with biochemical relapse. In the third hormone

refractory patient, BAY86-7548 failed to show multiple bone metastases evident on [^{18}F]-fluoromethylcholine PET/CT.

Conclusion:

BAY86-7548 PET/CT is a promising molecular imaging technique for detecting intraprostatic PCa.

Translational Relevance

Overexpression of bombesin receptors has been observed in several neoplastic diseases, including prostate cancer (PCa), thus offering a promising target for *in vivo* imaging. Anatomic imaging often fails to detect local disease with sufficient specificity for emerging focal therapies for PCa. Therefore, novel techniques showing the dominant intraprostatic lesion are becoming increasingly important. This study shows that ^{68}Ga -labeled DOTA-4-amino-1-carboxymethyl-piperidine-*D*-Phe-Gln-Trp-Ala-Val-Gly-His-Sta-Leu-NH₂-peptide (BAY86-7548) PET/CT detects organ-confined PCa with an accuracy of 83%, which is at least comparable to multiparametric MRI and PET/CT using radiolabeled choline or acetate. Autoradiography findings obtained from surgical specimens indicated that BAY86-7548 indeed detects bombesin receptor subtype 2 (gastrin-releasing peptide receptor, GRPr) positive lesions and could assist in planning of focal treatment of PCa.

Introduction

Prostate cancer (PCa) is the most frequently diagnosed cancer and the second most common cause of cancer deaths among men (1). Prostate specific antigen (PSA) and digital rectal examination are the first-line investigations in evaluating the risk of PCa while diagnosis is mainly based on transrectal ultrasound (TRUS) -guided biopsies. Due to low diagnostic accuracy of TRUS, many doctors prefer systematic biopsies for detection of PCa (2). However, about 25-35% of cancers are missed on first systematic biopsy (3, 4) and the Gleason score, which characterizes the malignant potential of PCa, is commonly underestimated (5). In addition, attempts to improve PCa detection by intensifying the biopsy technique have failed and seem to increase the risk of complications (6). Therefore, better imaging tools are needed to detect clinically significant cancer foci and to avoid unnecessary biopsies. Moreover, precise localization of cancer is needed to improve and further develop local prostate gland sparing therapies.

Multiparametric magnetic resonance imaging (MRI) has been shown to improve diagnostic accuracy in the evaluation of intraprostatic PCa (7). Nevertheless, due to different imaging protocols, technical factors and study populations, the variability in the reported sensitivities and specificities remains high. (7, 8).

Positron emission tomography (PET) is frequently used in oncology but its role in diagnosis of primary PCa is not well-established. The most common tracer, ^{18}F -labeled fluorodeoxyglucose (^{18}F -FDG), has a low sensitivity for detecting early PCa due to the low glucose consumption (9, 10), limiting the possibility to detect clinically localized disease. Other tracers, such as ^{18}F - or ^{11}C -labeled choline and ^{11}C -acetate, are used mainly for the diagnosis of recurrent (11-13) or metastatic (14) PCa. Their feasibility in primary diagnosis is limited due to uptake in benign tissue, such as benign prostatic hyperplasia (BPH) (15, 16).

⁶⁸Ga-labeled DOTA-4-amino-1-carboxymethyl-piperidine-*D*-Phe-Gln-Trp-Ala-Val-Gly-His-Sta-Leu-NH₂ (BAY86-7548) is a synthetic bombesin receptor antagonist, which targets gastrin-releasing peptide receptors (GRPr) (17). GRPr proteins are highly overexpressed in several human tumors, including PCa (18). Due to their low expression in BPH and inflammatory prostatic tissues (19, 20), imaging of GRPr has potential advantages over current choline- and acetate-based radiotracers. Indeed, preclinical studies using BAY86-7548 have shown a high and persistent tracer uptake in mice bearing PC-3 tumor xenografts, which represent androgen-independent human PCa with high GRPr expression (21).

The aim of this prospective, multi-site study was to investigate the safety, tolerability and accuracy of BAY86-7548 in detection of primary PCa and lymph node metastases in patients scheduled for radical retropubic or robot-assisted laparoscopic prostatectomy. In addition, feasibility of detecting recurrent PCa in comparison to [¹⁸F]-fluoromethylcholine, [¹¹C]-acetate PET/CT or MRI was examined in three patients with rising PSA after radical or palliative treatment. Finally, the potential of BAY86-7548 to study GRPr expression in human PCa was studied.

Materials and Methods

Patients and study design

Eleven patients (mean age, 63 years; range, 48–72 years) with histologically confirmed prostate adenocarcinoma, diagnosed through systematic TRUS-guided biopsies, and three patients (mean age, 67 years; range, 51–82 years) with biochemical recurrence of PCa were prospectively enrolled. Individual patient characteristics are presented in Table 1. Thirteen patients were studied in Turku, Finland and one in Zurich, Switzerland. Additional inclusion criteria for patients undergoing radical prostatectomy were presence of cancer in at least 20% of biopsy material and patient preference to undergo radical surgery including pelvic lymphadenectomy after discussion of the treatment options with the study urologist (E.K.). None of the patients studied in Turku had received any hormonal or radiation therapy while the patient in Zurich was in androgen-resistant phase after pelvic radiotherapy, several local palliative radiotherapies and antiandrogenic therapy. In addition, a multiparametric 3T MRI using surface coil was performed for three patients (no. 9, 11 and 12) and [^{11}C]-acetate PET/CT in three patients (no. 11, 12 and 13). The patient in Zurich (no. 14) underwent [^{18}F]-fluoromethylcholine PET/CT. Multiparametric 3T MRI consisted of anatomical T2- and T1-weighted images, dynamic contrast-enhanced MRI and diffusion-weighted imaging.

The study protocol was approved by the local ethics committees in Turku and Zurich as well as the respective authorities and each patient gave written informed consent for participation in the study. The entire study was conducted according to the guidelines of the Declaration of Helsinki.

Synthesis of BAY86-7548

The precursor, DOTA-4-amino-1-carboxymethylpiperidine-*D*-Phe-Gln-Trp-Ala-Val-Gly-His-Sta-Leu-NH₂ (BAY86-7547), was obtained from Bayer HealthCare Pharmaceuticals (Berlin, Germany). All the other reagents were purchased from commercial suppliers and were synthesis or analytical grade.

Turku. The radiosynthesis was performed with fully automated synthesis device (Modular Lab, Eckert & Ziegler Eurotope GmbH, Berlin, Germany). ⁶⁸Ga was obtained from a ⁶⁸Ge/⁶⁸Ga generator (IGG-100, 50 mCi (1850 MBq), Eckert & Ziegler Isotope Products, Valencia, CA, USA) by eluting the generator with 7 mL of 0.1 M HCl. The radioactive fraction of the ⁶⁸Ga eluate (1.6 mL) was collected and the HEPES-buffered BAY86-7547 (28 µg, 17 nmol) was added. The reaction mixture was incubated at 100–120°C for 12.5 min followed by SepPak purification, sterile filtration and formulation with sterile phosphate-buffered saline (PBS). The identity and the radiochemical purity of the product (BAY86-7548) were evaluated by radio-HPLC. The identity was confirmed by comparing the retention times of the peaks obtained from BAY86-7548 and BAY86-7547. The *in vitro* stability of BAY86-7548 was tested in formulation solution (PBS) by incubating for 2 h at room temperature followed by radio-HPLC analysis.

Zurich. The radiosynthesis was comparable to that in Turku except for the ⁶⁸Ga eluate, which was trapped onto a cation-exchange cartridge (Strata-X-C, Phenomenex). Then, 0.4 mL of 98% acetone/0.02 M HCl was used to elute ⁶⁸Ga from the cartridge. The peptide BAY86-7547 (28 µg, 17 nmol) and uric acid were dissolved in 2 mL 0.2 M sodium acetate buffer and prefilled into the reaction vessel. This was followed by incubation of the reaction mixture at 95°C for 6 min 40 sec and formulation and *in vitro* stability testing in saline instead of PBS. Otherwise, the procedures were similar.

BAY86-7548 PET/CT imaging

The patients were imaged in supine position using a GE Discovery VCT (Turku) or ST16 (Zurich) PET/CT Scanner (General Electric Medical Systems, Milwaukee, WI, USA). Low-dose CT protocol (120 kV, 10–80 mA, noise index 25, slice thickness 3.75 mm in Turku and 140 kV, 10–80 mA, noise index 11.75, slice thickness 3.75 mm in Zurich) was performed and also used for attenuation correction. A median dose of 147 MBq (range, 108–161 MBq) of BAY86-7548 was injected as an intravenous bolus. During imaging the vital signs were monitored including a 12-lead electrocardiogram, and blood and urine chemistry. The measured data were corrected for dead time, decay and photon attenuation and reconstructed into 256×256 matrix. Image reconstruction followed a fully 3D VUE Point GE algorithm incorporating random and scatter correction with two iterations and 28 subsets. The post filter was 3.00 mm FWHM (full-width at half-maximum) and the field of view diameter was 700 mm yielding to image pixel size of 3 mm. The final in-plane resolution of both PET/CT systems was 5 mm.

Surgical patients (n = 11). Urethral catheter was used in 9 (82%) patients in order to limit accumulation of BAY86-7548 in bladder and to allow better visualization of urethra on PET/CT images. Tracer injection was immediately followed by dynamic PET acquisition of the lower pelvic area over 60 min in 10 patients. A static whole-body emission scan (7 bed positions, 420 s per bed position) covering the whole torso in caudal to cephalic direction was then acquired 69 ± 3 min after tracer injection. In addition, 6 patients had a second static PET of pelvic area (1 bed position of 420 s duration) 102 ± 7 min after injection. Patient no. 1 had static PET emission scan covering pelvic area 58 min after injection immediately followed by whole-body imaging.

Biochemical recurrence (n = 3). Two patients with suspicion of recurrent PCa (no. 12 and 13) had static PET emission scan covering whole-body 58 min after tracer injection. The

third patient with suspicion of bone metastases (no. 14) received whole-body imaging starting 60 min from injection.

BAY86-7548 PET/CT image analysis

An experienced nuclear medicine physician (J.K.) and a medical student (I.J.) interpreted the PET/CT images in Turku in consensus. Both examiners were aware of the PCa diagnosis or suspicion of cancer recurrence, but were blinded to clinical and histopathological findings. PET/CT images in Zurich were interpreted by an experienced nuclear medicine physician (N.S.). In patients with primary PCa, a region-based analysis was used. The prostate gland was divided into three parts in superior-inferior axis. Each third was further divided into 4 quadrants (anterior, posterior, left, right). Presence of PCa on PET/CT images was defined as any mono- or multifocal uptake greater than adjacent background in more than one slice within the CT-defined prostate gland area. In addition to region-based analysis, lesion-based analysis was performed in which each abnormal focus was correlated with prostatectomy findings to define its histopathological nature. Finally, regions of interest (ROIs) were placed on visually identified abnormal foci as well as areas defined as BPH and normal prostate tissue of the peripheral zone based on histopathological findings from whole-mount prostatectomy samples. Maximum standardized uptake value (SUV_{max}) and mean standardized uptake value with a 60% threshold (SUV_{mean}) were determined in all ROIs. Tumors with the largest diameter of more than 0.5 cm were included into the analysis. The diagnostic accuracy of BAY86-7548 PET/CT was assessed using whole mount prostatectomy sections. In patients with biochemical recurrence, additional imaging modality was performed to clarify the findings of BAY86-7548 PET/CT.

Surgery

Open radical retropubic ($n = 2$) or robot-assisted laparoscopic prostatectomy ($n = 9$) and bilateral extended iliacal lymphadenectomy was performed 4 to 34 days after BAY86-7548 imaging. Preoperative risk of lymph node metastasis was estimated using Briganti nomograms (22). The surgeon (E.K.) was aware of the result of BAY86-7548 imaging and was encouraged to harvest especially the PET/CT positive lymph nodes. The routine area resected was defined as follows: Lateral border of excised fibrofatty tissue was pelvic wall and external and common iliac artery to the ureteral crossing, medial border was perivesical fat, inferior border was femoral canal and superior border was ureter. In addition, the fibrofatty tissue from both obturator fossa and next to internal iliac artery was removed.. Patient no. 3 had incomplete lymphadenectomy due to cardiopulmonary instability at the end of operation. Patient no. 8 showed suspicious metastatic lymph nodes outside routine lymphadenectomy area, just above aortic bifurcation on BAY86-7548 PET/CT and had also these nodes resected. These nodes were not detected on preoperative CT.

Histopathological analysis

Histologic slides were analyzed by two experienced pathologists (K.A., M.K.). After radical prostatectomy, the prostate glands were fixed in 10% buffered formalin for 24–48 hours. After fixation, the, left, right and anterior surfaces were inked with different colors to preserve the orientation of the prostate gland and to allow correlation with PET/CT images. Whole-mount axial macro-sections were obtained at 8-mm intervals transversely in a plane perpendicular to the long axis of the prostate gland in superior-inferior direction. The most apical macro-section was further sectioned in coronal orientation for easier evaluation of the capsular status of the inferior region. The first transversal section at the base was further sectioned in sagittal orientation for easier evaluation of the margin and seminal vesicles. Four μm whole-mount sections from each macro-section were stained with hematoxylin and eosin.

The presence and location of cancer foci, high-grade prostate intraepithelial neoplasm (HGPIN), prostatitis, BPH, capsular status and seminal vesicle invasion were determined. Gleason score was assessed as combination of the most common and the second most common type of Gleason grading for each tumor focus.

GRP receptor autoradiography

Fresh tissue samples of $1.5 \times 1.5 \times 0.5$ cm size for autoradiography (ARG) were taken from right and left lobe of prostate gland in 10 patients. Patient no. 2 had two fresh tissue samples from each lobe while the remaining patients had only one per each lobe. The samples were immediately frozen at -70°C . Cryostat sections ($20\text{ }\mu\text{m}$ thick) of these samples were processed for receptor ARG as described previously for other peptide receptors (22) using GRPr-specific [^{125}I]-Tyr⁴-bombesin as radioligand (23). Tissue sections were mounted on precleaned microscope slides and stored at -20°C for at least 3 days to improve adhesion of tissue to the slide. Sections were then processed according to Vigna et al. (23). They were first preincubated in 10 mM HEPES buffer (pH 7.4) for 5 min at room temperature followed by incubation in 10 mM HEPES, 130 mM NaCl, 4.7 mM KCl, 5 mM MgCl_2 , 1 mM ethyleneglycol-bis (β -aminoethylether)-N-N9-tetraacetic acid, 0.1% BSA, 100 mg/mL bacitracin (pH 7.4), and approximately 100 pM [^{125}I]-Tyr⁴-bombesin-14 (81.4 TBq/mmol; PerkinElmer, Turku, Finland) in the presence or absence of 1 mM bombesin for 1 h at room temperature. After incubation, the sections were washed four times for 2 min in 10 mM HEPES with 0.1% BSA (pH 7.4) at 4°C . Finally, the slides were rinsed twice for 5 sec at 4°C in distilled water, dried at room temperature, and placed in apposition to imaging plates (Fuji Imaging Plate BAS-TR2025, Fuji Photo Film Co., Ltd., Tokyo, Japan) for 14 days for scanning with the Fuji Analyzer FLA-5100. Sections were stained with hematoxylin-eosin to localize the areas of BPH, PCa and HGPIN.

Statistical analysis

Statistical analysis was performed with SAS, version 9.3 (SAS Institute Inc., Cary, NC, USA). SUV measurements were compared using Bonferroni multiple comparison test (24). Normal distributions were assessed by the Kolmogorov and Smirnov method. A p-value below 0.01 was considered to be statistically significant.

Results

Patients' clinical findings are summarized in Table 1. No drug-related adverse events were associated with BAY86-7548 and all patients tolerated the imaging procedure well. The mean PSA level of patients with primary PCa was 18 ± 11 ng/mL (range, 6.2–45.0 ng/mL), while the three patients with biochemical recurrence of PCa had PSA levels of 0.36, 4.7 and 282 ng/mL. Based on histopathological analysis of whole-mount prostatectomy samples, 26 tumor foci were identified in 11 patients, with 19 (73%) of these foci larger than 0.5 cm.

BAY86-7548 demonstrated fast excretion through kidneys with 25% of injected radioactivity dose observed in urine 30 min after injection. Plasma pharmacokinetics, whole-body distribution, metabolism and radiation dosimetry of BAY86-7548 in healthy men have been previously described (25). The highest radioactivity uptake was detected in the urinary bladder and pancreas, which is in the line with the known expression of GRPr and previous preclinical studies with RM2 peptide (21). Maximum peak uptake of the total injected radioactivity was seen in the urinary bladder and liver, 36% and 19%, respectively.

Preparation of BAY86-7548

The radiopharmaceutical BAY86-7548 was obtained with a moderate yield (440 ± 120 MBq, $n = 13$). Radioactivity concentration and specific radioactivity at end of synthesis (EOS) were 44 ± 13 MBq/ml and 26 ± 7 GBq/ μ mol, respectively. Radiochemical purity was at least 97% and the difference between retention times of HPLC peaks obtained from BAY86-7547 and BAY86-7548 was 0.19 ± 0.07 min. The tracer remained radiochemically stable for 2 hours in formulation solution at room temperature; radiochemical purity was $98 \pm 0\%$ at 1 hour after EOS and $98 \pm 1\%$ at 2 hours after EOS (mean \pm SD, $n = 3$). Every injected batch of BAY86-7548 fulfilled the release criteria.

Diagnostic accuracy of cancer detection

Region-based analysis of BAY86-7548 PET/CT findings in 132 regions, of which 57 (43%) contained cancer according to histopathological analysis, revealed 63 regions as positive and 69 as negative. Using histology as gold standard, 49 of these were considered true-positive and 61 true-negative, yielding a sensitivity, specificity, and accuracy of 89%, 81%, 83%, respectively. Lesion-based analysis of BAY86-7548 PET/CT revealed 15 true-positive tumor lesions, 6 false-positive lesions, and 4 false-negative lesions resulting in a sensitivity of 79%. The 6 false-positive intraprostatic lesions were determined to be BPH based on whole mount prostatectomy sections. BAY86-7548 PET/CT successfully detected all dominant lesions except one anterior lesion. However, another smaller peripheral zone tumor of the same patient (no. 2) was detected. Both of the lesions had the Gleason score of 3+4.

Detection of lymph node metastasis

Primary PCa with at least one metastatic lymph node was present in three (27%) out of eleven patients undergoing prostatectomy with lymph node dissection. In total, 135 lymph nodes were histopathologically analyzed with 10 showing the presence of metastatic PCa. Per patient sensitivity was 67% and per node sensitivity was 70% for BAY86-7548 PET/CT. The sizes of the three BAY86-7548 negative metastases were 6 mm (patient no. 1, left iliac node), 5 mm and 5 mm (patient no. 6, two right iliac lymph nodes). Patient no. 6 had in addition one correctly detected metastatic left iliac node (size 11 mm). Two normal-sized lymph nodes (less than 10mm) were removed from patient no. 8 above the aortic bifurcation based on guidance of BAY86-7548 PET/CT (see Surgery). Both of these were histopathologically confirmed as PCa metastases (Figure 1).

Quantitative analysis

The average SUV_{max} and SUV_{mean} were 6.6 ± 4.7 , 5.1 ± 3.7 , respectively, for histologically confirmed cancer foci as measured 60–70 min after injection. These values were different from the SUV_{max} and SUV_{mean} of BPH (2.4 ± 1.5 , 1.8 ± 1.2 , respectively) and normal tissue of peripheral zone (1.3 ± 1.0 , 1.0 ± 0.9 , respectively) ($p < 0.01$ for all comparisons). No significant difference in SUV_{max} and SUV_{mean} of BPH and normal tissue of peripheral zone was observed. See Figure 2.

Results of autoradiography

PCa was present in 15 (68%) autoradiography sections. All lesions were positive by autoradiography. BPH nodules in two tissue sections and HGPIN lesion in one tissue section were positive, indicating the presence of GRPr expression (Figure 3).

Patients with clinical suspicion of recurrent disease

BAY86-7548 PET/CT successfully detected recurrence of PCa in the two hormone-naïve patients with biochemical recurrence (no. 12 and 13). The findings were in concordance with [^{11}C]-acetate PET/CT and 3T MRI in prostate bed in patient no. 12. By contrast, both [^{11}C]-acetate PET/CT and diffusion-weighted MRI suggested the presence of metastatic parailiac lymph node while BAY86-7548 PET/CT did not show any pathological uptake in this region. The patient subsequently received radiotherapy to PET and MRI positive prostatic bed and parailiac nodes bilaterally. In a repeated [^{11}C]-acetate PET/CT 3 months from radiotherapy, PSA was 0.068 and the prostate bed had turned [^{11}C]-acetate negative while the parailiac lymph node was still positive. On CT, this node measured 6 mm and remained unchanged before and after radiotherapy in spite of rapid decrease in serum PSA. In patient no. 13, BAY86-7548 was positive in one iliac and one mediastinal node, which were similarly

positive on [^{11}C]-acetate. In addition, [^{11}C]-acetate showed several positive lymph nodes in unconventional locations such as axillary, parasternal and inguinal regions. The single patient imaged in Zurich (no. 14) had multiple [^{18}F]-fluoromethylcholine positive bone metastases and his BAY86-7548 PET/CT was totally negative.

Discussion

With the evolution of local and minimally invasive therapies for PCa, such as focal radiotherapy and high-intensity focused ultrasound, a pressure to develop better diagnostic tools to detect primary PCa is evident. Currently, multiparametric MRI is being increasingly utilized in imaging of local PCa to plan focal therapies (7, 8). Combination of functional and anatomical information using hybrid PET/MRI imaging can be a powerful technique provided that the applied tracer and the chosen MRI acquisition protocol are optimized for each patient individually.

Because none of the currently available positron emitting tracers can reliably detect early PCa or identify the extent of intraprostatic disease, there is a demand for more specific tracers. An ideal tracer would detect the dominant PCa lesion and differentiate cancer from BPH and inflammatory lesions. We studied a novel ^{68}Ga -labeled bombesin antagonist BAY86-7548 to translate the encouraging pre-clinical findings (21) to identical results in patients scheduled for radical prostatectomy or with biochemical recurrence. We were specifically interested in the uptake of BAY86-7548 in intraprostatic lesions and in the potential of the peptide tracer to detect metastatic lymph nodes. By selecting ^{68}Ga as the radionuclide, we were able to perform the study without access to cyclotron.

The potential of ^{68}Ga -labeled peptides to target tumor receptors has been previously demonstrated in the case of somatostatin receptor imaging. Due to their higher sensitivity and better biodistribution properties (26, 27), [^{68}Ga]-DOTATOC, [^{68}Ga]-DOTANOC, and [^{68}Ga]-DOTATATE are used for diagnosis of neuroendocrine tumors and are gradually replacing conventional gamma emitting radioisotope techniques in Europe. In general, peptides provide excellent characteristics for PET imaging due to their easy synthesis, fast and specific targeting features and rapid clearance from the body mainly via the renal pathway. Much like

somatostatin receptors, peptides targeting G-protein coupled receptors are effectively accumulating in tumors *in vivo*.

The GRPr, also named bombesin receptor subtype 2, is a G-protein coupled seven-transmembrane receptor belonging to the bombesin receptor family with four subtypes (for review, see (17)). GRPr proteins are highly overexpressed in several human tumors, including PCa, breast cancer, small cell lung cancer (SCLC) and non-SCLC, as well as renal cell cancer (18). Our results with radiolabeled bombesin antagonist (BAY86-7548) indicate that this tracer could be more PCa-specific than imaging with [^{18}F]-, [^{11}C]-choline or [^{11}C]-acetate, which generally depict lipid metabolism and accumulate also in BPH and inflammatory conditions. Bombesin receptor antagonists may be preferable to agonists for tumor imaging due to higher tumor uptake and longer tumor washout time (28). In addition, bombesin receptor antagonists have reduced physiologic activity and radioactivity accumulation at physiologic GRPr targets, which potentially imply fewer side effects (28).

Despite the variety of bombesin compounds synthesized and evaluated, none have been systematically evaluated in patients with PCa. The study by Van de Wiele et al. using [$^{99\text{m}}\text{Tc}$]-527RP scintigraphy targeting GRPr, had only four patients with metastatic PCa. One of these patients had specific uptake of [$^{99\text{m}}\text{Tc}$]-527RP in PCa metastasis (29). In the current study, ^{68}Ga -labeled bombesin antagonist BAY86-7548 had encouraging results in detection of primary PCa by having an accuracy of 83% for detection of the organ-confined disease. Notably, a significant difference was observed in SUV between cancerous and hyperplastic lesions. This is an encouraging finding, since non-specific uptake in benign prostatic lesions is one of the major limitations of radiolabeled choline or acetate. However, fusion of anatomical MRI with [^{18}F]-, [^{11}C]-choline or [^{11}C]-acetate PET can only partly overcome this limitation (30). Apart from some small cancer foci, 10 out of 11 dominant lesions were detected positive with BAY86-7548.

In detection of lymph node metastases a sensitivity of 70% was observed. Although limited, it is not inferior to that seen in [^{18}F]-fluoromethylcholine or [^{11}C]-acetate PET/CT imaging or multiparametric MRI. In addition to the lack of expression of GRPr in a particular lesion, there are two explanations for this less-than-optimal sensitivity. Firstly, small and diffusely growing metastatic deposits or primary foci can be missed if the tumor-specific uptake is low due to partial volume effects. Secondly, the physical characteristics of ^{68}Ga with its average positron range between 2–3 mm are less ideal than those of the more widely used radionuclides, such as ^{18}F (31). Due to the low number of patients with biochemical recurrence, the potential of BAY86-7548 in diagnosis of recurrent PCa remained inconclusive. Finally, most of our patients undergoing a surgery belonged to the high clinical risk group with high risk of lymph node metastasis. This resulted in relatively high percentage (43%) of regions containing cancer according to histopathological analysis and a selection bias embedded to the study inclusion criteria could not be completely avoided. Since whole-mount axial macro-sections were obtained at 8-mm intervals, some small PCa lesions could have been missed and the diameter of larger cancer lesions could have been underestimated. It is well known that precise correlation of PCa location on whole-mount prostatectomy to PET/CT and MRI is relative difficult (32). Anatomical landmarks, such as urethra, were used to enable the correlations of whole-mount prostatectomy to PET/CT images. Although no cross-calibration of the two PET/CT scanners was performed, the consequences are considered minimal since only one patient was studied using a different PET/CT scanner.

Although radiolabeled choline or acetate remain the most commonly used tracers for imaging of biochemical relapse, these tracers have shown only limited accuracy in detection of primary PCa (15, 16). In a recent study including 39 patients undergoing radical prostatectomy, multiparametric MRI showed a sensitivity of 82% for detection of PCa lesions greater than 0.5 cm while the sensitivity of [^{11}C]-acetate PET/CT was only 62% (33).

Similarly, MRI including MR spectroscopy has been shown to outperform [^{11}C]-choline PET/CT in evaluation of primary disease (34) and multiple studies have demonstrated low specificity of radiolabeled choline or acetate for PCa imaging due to uptake in BPH (15, 16, 33). Currently, none of these ^{18}F - or ^{11}C -labeled tracers, which are metabolized in the phospholipid synthesis pathway, can be recommended for evaluation of primary PCa (35). Therefore, the 83% accuracy of BAY86-7548 PET/CT observed in this study is indeed encouraging. When combined with multiparametric MRI, BAY86-7548 PET/CT may result in sufficient diagnostic performance to allow focal treatment of intraprostatic lesions of PCa.

Despite the relatively small number of patients, we have demonstrated the feasibility of BAY86-7548 PET/CT for detection of organ-confirmed PCa. Our histopathological and autoradiography analyses indicated that ^{68}Ga -labeled bombesin antagonist BAY86-7548 had high PCa binding specificity with significantly higher uptake in PCa compared to benign tissue. BAY86-7548 was well tolerated by all patients. This new tracer could be more accurate in detection of primary and recurrent PCa than previously used positron emitting tracers, although its feasibility in imaging of metastatic disease requires further optimization.

Acknowledgments

The authors thank the staff at Turku PET Centre and research nurses at the Department of Oncology and Radiotherapy and Clinical Research Service Turku (CRST), University of Turku, for their assistance. The authors also thank Piramal Imaging GmbH (Berlin, Germany) for providing the BAY86-7548 (^{68}Ga]-DOTA-RM2), Mr. Jaakko Liippo for his help in preparing the images and Aurexel Ltd for editorial support. Part of the study was presented at the 25th European Association of Nuclear Medicine (EANM) Annual Meeting in Milan on October 27-31, 2012 and the authors wish to thank the EANM organizers for selecting the study as a recipient of the EANM Marie Curie Award.

References

- (1) Siegel R, Naishadham D, Jemal A. Cancer statistics, 2012. *CA Cancer J Clin* 2012;62:10-29.
- (2) Halpern EJ, Frauscher F, Strup SE, Nazarian LN, O'Kane P, Gomella LG. Prostate: high-frequency Doppler US imaging for cancer detection. *Radiology* 2002;225:71-7.
- (3) Djavan B, Ravery V, Zlotta A, Dobronski P, Dobrovits M, Fakhari M, et al. Prospective evaluation of prostate cancer detected on biopsies 1, 2, 3 and 4: when should we stop? *J Urol* 2001;166:1679-83.
- (4) Roehl KA, Antenor JA, Catalona WJ. Serial biopsy results in prostate cancer screening study. *J Urol* 2002;167:2435-9.
- (5) Rajinikanth A, Manoharan M, Soloway CT, Civantos FJ, Soloway MS. Trends in Gleason score: concordance between biopsy and prostatectomy over 15 years. *Urology* 2008;72:177-82.
- (6) Simon J, Kuefer R, Bartsch G, Jr., Volkmer BG, Hautmann RE, Gottfried HW. Intensifying the saturation biopsy technique for detecting prostate cancer after previous negative biopsies: a step in the wrong direction. *BJU Int* 2008;102:459-62.
- (7) Hoeks CM, Barentsz JO, Hambrock T, Yakar D, Somford DM, Heijmink SW, et al. Prostate cancer: multiparametric MR imaging for detection, localization, and staging. *Radiology* 2011;261:46-66.
- (8) Hricak H, Choyke PL, Eberhardt SC, Leibel SA, Scardino PT. Imaging prostate cancer: a multidisciplinary perspective. *Radiology* 2007;243:28-53.

- (9) Liu IJ, Zafar MB, Lai YH, Segall GM, Terris MK. Fluorodeoxyglucose positron emission tomography studies in diagnosis and staging of clinically organ-confined prostate cancer. *Urology* 2001;57:108-11.
- (10) Takahashi N, Inoue T, Lee J, Yamaguchi T, Shizukuishi K. The roles of PET and PET/CT in the diagnosis and management of prostate cancer. *Oncology* 2007;72:226-33.
- (11) Sandblom G, Sorensen J, Lundin N, Haggman M, Malmstrom PU. Positron emission tomography with ^{11}C -acetate for tumor detection and localization in patients with prostate-specific antigen relapse after radical prostatectomy. *Urology* 2006;67:996-1000.
- (12) Oyama N, Miller TR, Dehdashti F, Siegel BA, Fischer KC, Michalski JM, et al. ^{11}C -acetate PET imaging of prostate cancer: detection of recurrent disease at PSA relapse. *J Nucl Med* 2003;44:549-55.
- (13) Wachter S, Tomek S, Kurtaran A, Wachter-Gerstner N, Djavan B, Becherer A, et al. ^{11}C -acetate positron emission tomography imaging and image fusion with computed tomography and magnetic resonance imaging in patients with recurrent prostate cancer. *J Clin Oncol* 2006;24:2513-9.
- (14) Kotzerke J, Volkmer BG, Glatting G, van den Hoff J, Gschwend JE, Messer P, et al. Intraindividual comparison of [^{11}C]acetate and [^{11}C]choline PET for detection of metastases of prostate cancer. *Nuklearmedizin* 2003;42:25-30.
- (15) Souvatzoglou M, Weirich G, Schwarzenboeck S, Maurer T, Schuster T, Bundschuh RA, et al. The sensitivity of [^{11}C]choline PET/CT to localize prostate cancer depends on the tumor configuration. *Clin Cancer Res* 2011;17:3751-9.

- (16) Jambor I, Borra R, Kemppainen J, Lepomaki V, Parkkola R, Dean K, et al. Functional Imaging of Localized Prostate Cancer Aggressiveness Using ^{11}C -Acetate PET/CT and ^1H -MR Spectroscopy. *J Nucl Med* 2010;51:1676-83.
- (17) Jensen RT, Battey JF, Spindel ER, Benya RV. International Union of Pharmacology. LXVIII. Mammalian bombesin receptors: nomenclature, distribution, pharmacology, signaling, and functions in normal and disease states. *Pharmacol Rev* 2008;60:1-42.
- (18) Reubi JC, Wenger S, Schmuckli-Maurer J, Schaer JC, Gugger M. Bombesin receptor subtypes in human cancers: detection with the universal radioligand (^{125}I)-[D-TYR(6), beta-ALA(11), PHE(13), NLE(14)] bombesin(6-14). *Clin Cancer Res* 2002;8:1139-46.
- (19) Markwalder R, Reubi JC. Gastrin-releasing peptide receptors in the human prostate: relation to neoplastic transformation. *Cancer Res* 1999;59:1152-9.
- (20) Beer M, Montani M, Gerhardt J, Wild PJ, Hany TF, Hermanns T, et al. Profiling gastrin-releasing peptide receptor in prostate tissues: clinical implications and molecular correlates. *Prostate* 2012;72:318-25.
- (21) Mansi R, Wang X, Forrer F, Waser B, Cescato R, Graham K, et al. Development of a potent DOTA-conjugated bombesin antagonist for targeting GRPr-positive tumours. *Eur J Nucl Med Mol Imaging* 2011;38:97-107.
- (22) Reubi JC, Kvols LK, Waser B, Nagorney DM, Heitz PU, Charboneau JW, et al. Detection of somatostatin receptors in surgical and percutaneous needle biopsy samples of carcinoids and islet cell carcinomas. *Cancer Res* 1990;50:5969-77.

- (23) Vigna SR, Mantyh CR, Giraud AS, Soll AH, Walsh JH, Mantyh PW. Localization of specific binding sites for bombesin in the canine gastrointestinal tract. *Gastroenterology* 1987;93:1287-95.
- (24) DeGroot M. H., Schervish M. J. Kolmogorov-Smirnov Tests. In: *Probability and Statistics*, Pearson, 2011. p. 657-58
- (25) Roivainen A, Kahkonen E, Luoto P, Borkowski S, Hofmann B, Jambor I, et al. Plasma Pharmacokinetics, Whole-Body Distribution, Metabolism, and Radiation Dosimetry of ⁶⁸Ga Bombesin Antagonist BAY86-7548 in Healthy Men. *J Nucl Med* 2013.
- (26) Kumar R, Sharma P, Garg P, Karunanithi S, Naswa N, Sharma R, et al. Role of ⁶⁸Ga-DOTATOC PET-CT in the diagnosis and staging of pancreatic neuroendocrine tumours. *Eur Radiol* 2011;21:2408-16.
- (27) Ambrosini V, Campana D, Bodei L, Nanni C, Castellucci P, Allegri V, et al. ⁶⁸Ga-DOTANOC PET/CT clinical impact in patients with neuroendocrine tumors. *J Nucl Med* 2010;51:669-73.
- (28) Cescato R, Maina T, Nock B, Nikolopoulou A, Charalambidis D, Piccand V, et al. Bombesin receptor antagonists may be preferable to agonists for tumor targeting. *J Nucl Med* 2008;49:318-26.
- (29) Van de Wiele C, Dumont F, Vanden Broecke R, Oosterlinck W, Cocquyt V, Serreyn R, et al. Technetium-99m RP527, a GRP analogue for visualisation of GRP receptor-expressing malignancies: a feasibility study. *Eur J Nucl Med* 2000;27:1694-9.

- (30) Jambor I, Borra R, Kemppainen J, Lepomaki V, Parkkola R, Dean K, et al. Improved detection of localized prostate cancer using co-registered MRI and ^{11}C -acetate PET/CT. *Eur J Radiol* 2012;81:2966-72.
- (31) Kemerink GJ, Visser MG, Franssen R, Beijer E, Zamburlini M, Halders SG, et al. Effect of the positron range of ^{18}F , ^{68}Ga and ^{124}I on PET/CT in lung-equivalent materials. *Eur J Nucl Med Mol Imaging* 2011;38:940-8.
- (32) Meyer C, Ma B, Kunju LP, Davenport M, Piert M. Challenges in accurate registration of 3-D medical imaging and histopathology in primary prostate cancer. *Eur J Nucl Med Mol Imaging* 2013.
- (33) Mena E, Turkbey B, Mani H, Adler S, Valera VA, Bernardo M, et al. ^{11}C -Acetate PET/CT in Localized Prostate Cancer: A Study with MRI and Histopathologic Correlation. *J Nucl Med* 2012.
- (34) Testa C, Schiavina R, Lodi R, Salizzoni E, Corti B, Farsad M, et al. Prostate cancer: sextant localization with MR imaging, MR spectroscopy, and ^{11}C -choline PET/CT. *Radiology* 2007;244:797-806.
- (35) Picchio M, Giovannini E, Messa C. The role of PET/computed tomography scan in the management of prostate cancer. *Curr Opin Urol* 2011;21:230-6.

Table 1. Patient characteristics

Patient	Age	Injected radio-activity	Post-operative TNM	Prostate gland weight	Gleason	Score _d	PSA at imaging	Preoperative risk of N+ disease	No. of PCa lesions	Size of dominant lesion	Proportion of cancer in prostate gland	No. of metastatic / recovered lymph nodes	Setting _a
					ARG _c	Final							
no.	(yrs)	(MBq)		(g)	right/left		(ng/mL)	(%)		(mm)	(%)		
1	62	161	T3bN1	54	0/3+4	4+3	16	30	2	17	30	1/15	P
2	57	160	T3aN0	59	3+3/3+4	3+4	6.9	7	3	16	30	0/14	P
3	72	150	T3bN0	152	3+3/3+3	4+3	45	28	2	26	20	0/3	P
4	69	159	T3bN0	55	0/4+4	3+4	21	60	1	19	20	0/7	P
5	63	154	T3aN0	47	3+4/3+3	4+3	6.2	17	2	16	20	0/13	P
6	62	153	T3bN1	35	3+3+4+4	4+4	15	22	3	12	20	3/13	P
7	64	148	T2cN0	32	3+4/4+3	3+4	17	22	1	35	20	0/20	P
8	66	146	T4N1M1	54	5+4/5+4	5+4	14	33	1	32	60	6/17	P
9	66	158	T3aN0	101	0/0	4+3	13	26	2	12	7	0/8	P
10	48	147	T2cN0	32	0/3+4	3+4	10	16	1	22	25	0/15	P
11	64	129	T3aN0	66	N/A	4+4	29	78	1	20	10	0/10	P
12	52	143	T3bN0M0	N/A	N/A	4+4	0.36	N/A	N/A	N/A	N/A	N/A	R
13	67	108	T2cN0M0	N/A	N/A	4+5	4.7	N/A	N/A	N/A	N/A	N/A	R
14	82	152	T2N1M0	N/A	N/A	2+3	282	N/A	N/A	N/A	N/A	N/A	R
Mean	64	147											
SD	8	15											

_a - P, primary cancer, R, recurrence; _b - N/A, not applicable; _c - ARG, autoradiography; _d - Final Gleason score is based on the whole mount prostatectomy while ARG Gleason score is from the particular tissues section used for ARG.

Figure legends

Figure 1. Coronal (A) and axial views (B,C) of BAY86-7548 PET/CT in patient no. 8 with PCa metastasis to multiple lymph nodes. Two normal-sized (less than 10 mm) nodes above the aortic bifurcation indicated with red arrow showed increased uptake of tracer, SUV_{max} 6.2 and 6.3. In addition, one left parailiac node, SUV_{max} 12.7, (B) and two right parailiac nodes, SUV_{max} 6.1 and 4.7, (C) showed increased uptake of BAY86-7548. These five lymph nodes were histologically confirmed as metastases at surgery. Green arrows point to ureters, which can be easily distinguished on anatomic CT. Images are scaled to SUV, with a minimum at 0 and maximum at 5.

Figure 2. Maximum (A) and mean (B) standardized uptake value (SUV) of BAY86-7548 in carcinoma, benign prostatic hyperplasia (BPH) and normal prostate gland tissue in 11 patients scheduled for radical prostatectomy. Significantly higher uptake expressed as SUV_{max} and SUV_{mean} of cancer foci was found compared to both BPH and normal tissue of peripheral zone. N.S. –not significant

Figure 3. BAY86-7548 PET/CT (A) of patient no. 10 showing uptake in the left lobe of prostate gland in the area of cancer based on whole mount prostatectomy sample (B - tumor is outlined in blue. (Bar, 1 cm). Autoradiography showed presence of GRPr in the section taken from the left lobe (D upper part. Bar, 1 cm) in the area of cancer (C upper part - tumor is outlined in blue. Bar, 1 cm), while only small areas of high-grade prostate intraepithelial neoplasm (HGPIN) in the section taken from the right lobe had positive activity (C, D lower part - red arrow points to the area of HGPIN. Bar, 1 cm). The presence of 1 mM

bombesin blocked uptake of [^{125}I]-Tyr⁴-bombesin-14 in the sections from left (D upper right part) and right (D lower right part) lobe. BAY86-7548 PET/CT image is scaled to SUV, with a minimum at 0 and maximum at 5.

Figure 4. The uptake of BAY86-7548 in patient no. 3 was localized in the peripheral (yellow arrow in A) and central zone (red arrow in A). These areas coincide well with cancer (outlined in blue) on corresponding prostatectomy sections (B - Bar, 1 cm). The large BPH nodules in the central zone did not show uptake of BAY86-7548. Black arrow points to urinary activity in a urethral catheter. The weight of the prostate gland immediately after prostatectomy was 152 g. Image is scaled to SUV, with a minimum at 0.5 and maximum at 5.

Figure 5. Pre-operative fusion of diffusion-weighted imaging ($b = 750 \text{ s/mm}^2$) with T2-weighted MRI (A), BAY86-7548 PET/CT (B) and [^{11}C]-acetate PET/CT (C) showed suspicious presacral metastatic lymph node in patient no. 11. BAY86-7548 SUV_{max} of the node was 2.0. Unfortunately, the node could not be accessed during robotic prostatectomy and remained positive on post-surgical [^{11}C]-acetate PET/CT (D) as did the patient's PSA (1.9). The preoperative [^{11}C]-acetate SUV_{max} of the suspicious node was 2.5 while post-surgical was 6.2. Subsequently endocrine therapy was started. Please note uptake of [^{11}C]-acetate in pelvic muscles not seen in BAY86-7548 PET/CT images. BAY86-7548 image is scaled to SUV, with a minimum at 0 and maximum at 5 while [^{11}C]-acetate images C and D are scaled to SUV, with a minimum at 0, 0 and maximum at 3.6, 10.9, respectively.

Figure 1

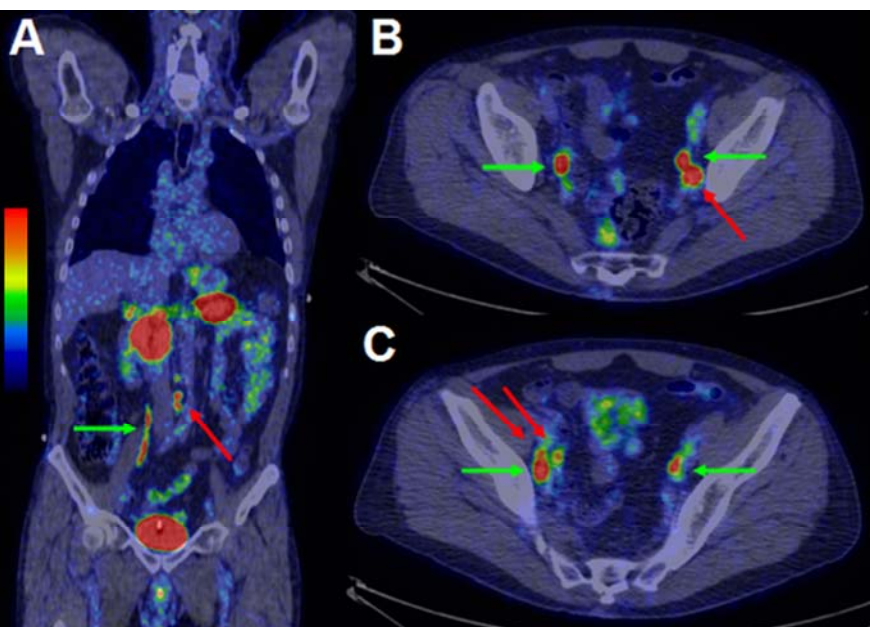


Figure 2

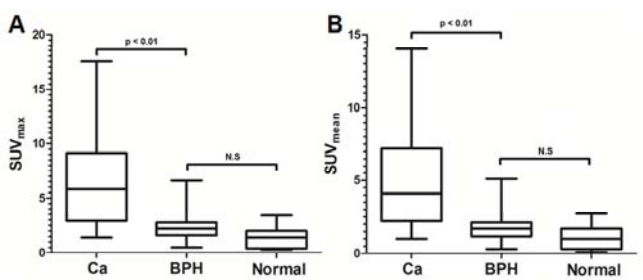


Figure 3

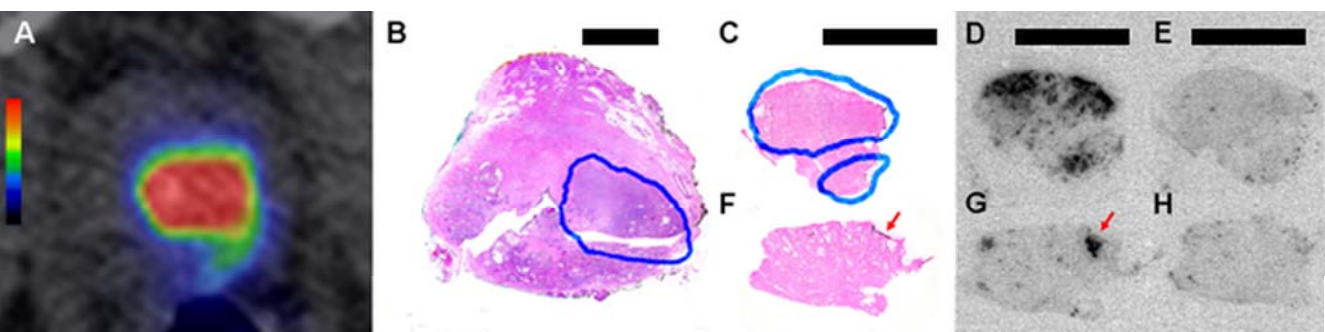


Figure 4

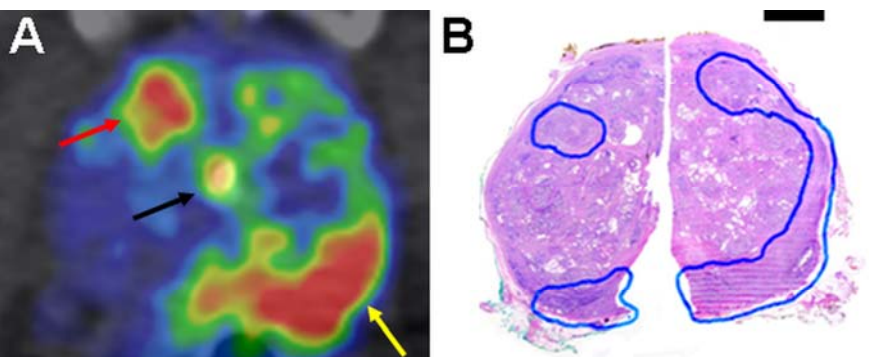


Figure 5

